Polymer 51 (2010) 3249–3261

Contents lists available at ScienceDirect

Polymer

journal homepage: www.elsevier.com/locate/polymer

Mechanistic aspects of sonochemical copolymerization of butyl acrylate and methyl methacrylate

Suresh Kanmuri, Vijayanand S. Moholkar*

Department of Chemical Engineering, Indian Institute of Technology Guwahati, Guwahati 781 039, Assam, India

ARTICLE INFO

Article history:
Received 4 February 2010
Received in revised form
7 May 2010
Accepted 7 May 2010
Available online 31 May 2010

Keywords:
Sonochemistry
Cavitation
Emulsion polymerization

ABSTRACT

This paper attempts to get a physical insight into the sonochemical emulsion copolymerization using butyl acrylate (BA) and methyl methacrylate (MMA) as model monomers at low to moderate ultrasound intensity. The principal physical mechanism underlying beneficial effects of ultrasound on emulsion polymerization system is cavitation, which affects the system in both chemical (i.e. generation of radicals that can initiate/propagate polymerization process) as well as physical (i.e. emulsification of reaction mixture) way. By taking dual approach of coupling experiments with simulations of cavitation bubble dynamics, we have tried to justify the trends in experiments results. The role of cavitation in the present study is found to be only physical. Quite interestingly, the chemical effect of cavitation is found to have no role to play. Reactivity ratios of both monomers for applied experimental conditions have been found to be less than 1, which hints at moderately alternating behavior of copolymerization. Theoretically calculated copolymer composition using the reactivity ratios of copolymers matched well with experimental values. The copolymer composition for all monomer feed ratios is rich in MMA, due to higher reactivity of MMA than BA. The molecular weight of the copolymer reduced with greater fraction of MMA in the reaction mixture. This effect is attributed to nature of termination of the BA (i.e., combination) and MMA (i.e., disproportionation) monomer radicals.

1. Introduction

Beneficial effect of ultrasound on polymerization and copolymerization reactions is known for more than half a century. Distinct merits of the sonochemical route for emulsion polymerization include faster polymerization at lower bulk liquid temperatures offering control over polydispersity, tacticity and molecular weight of the product. In some cases, ultrasound irradiation also eliminates need of chemical initiator and co-stabilizer [1,2]. Sonochemical polymerization was first reported in the 1950s by Lindstrom and Lamm [3] and Henglein [4,5]. Past couple of decades has seen extensive research in this area and voluminous literature on study of sonochemical polymerization of variety of monomers such as methyl methacrylate, butyl acrylate, vinyl acetate and styrene have been published [6–17]. Copolymerization of various monomers has also been studied with application of ultrasound. Zheng et al. [18] have studied ultrasonically initiated emulsion copolymerization of styrene and a cationic polymerizable surfactant (methacryloxyethyl dodecydimethyl ammonium bromide, C(12)N(+)) to prepare high purity copolymer nanolatex. Bradley et al. [19] have studied ultrasonically initiated batch miniemulsion copolymerization of MMA and BA with different monomer ratios. They have also attempted to predict the composition of the resulting copolymer with model TRISEPS (Trimonomeric Seeded Emulsion Polymerization Simulation). Fujiwara and Izutsu [20] have studied mechanochemical block copolymerization in heterogeneous systems of poly(vinyl chloride) with vinyl acetate by ultrasonic irradiation at 60 °C. Zhang et al. [21] have studied ultrasonically irradiated emulsion copolymerization of styrene and surfmer in presence of a polymeric surfactant. Yin and Chen [22] have studied the polymerization mechanism of ultrasonically initiated emulsifier–free emulsion copolymerization of BA and acrylamide (AM). Yan et al. [23] have studied synthesis of copolymer of styrene with acrylic acid by random emulsion copolymerization under ultrasonic irradiation without any volatile organic solvent or emulsifier. Other major contributions in the area of sonochemical copolymerization include those of Isayev [24], Bahattab and Stoffer [25], Bahattab et al. [26], Liu et al. [27], Koda et al. [28], Fujiwara et al. [29], Chen et al. [30] and Price et al. [31].

The reaction mixture in emulsion copolymerization is essentially a liquid–liquid heterogeneous system. Influence of ultrasound on such systems is of both physical and chemical nature. It needs to be mentioned that ultrasound manifests its effects through phenomenon of cavitation, which is nucleation, growth and transient collapse of tiny air/vapor bubbles which is driven by the pressure variation in

* Corresponding author. Fax: +91 361 258 2291.
E-mail address: vmoholkar@iitg.ac.in (V.S. Moholkar).

0032-3861/$ – see front matter © 2010 Elsevier Ltd. All rights reserved.
doi:10.1016/j.polymer.2010.05.011

the bulk liquid medium during passage of ultrasound waves [32,33]. The principal physical effect of cavitation phenomenon is formation of fine emulsion of the two liquids as a consequence of intense microturbulence and shock waves generated during radial motion of cavitation bubble. Typical size of droplets in this emulsion ranges between 50 and 500 nm as revealed by various studies mentioned above. Formation of such fine emulsion creates enormous interfacial area for reaction due to which the kinetics of polymerization shows significant acceleration. Principal chemical effect of cavitation is generation of radicals such as H•, •OH, $HO•_2$ and O• [34,35]. These radicals are generated due to dissociation of vapor molecules entrapped in the cavitation bubble during extreme conditions of temperature and pressure (~500 bar and 5000 K) reached at its transient adiabatic collapse [36–39]. These radicals can react with the monomer molecules to generate monomer radicals that can initiate, propagate and terminate polymerization reaction.

Most of the earlier studies in sonochemical copolymerization [18–31] are of experimental nature and little attempt is devoted to correlate the characteristic features of the copolymerization to cavitation bubble dynamics, which is the principal physical phenomenon underlying physical and chemical effects of ultrasound. In our previous paper [40], we attempted to establish the physical mechanism of emulsion homo-polymerization. In this paper, we extend our analysis to copolymerization system. Our approach is similar to our previous study [40], i.e. coupling experimental results to the simulations of cavitation bubble dynamics using a mathematical model. We have chosen copolymerization of BA and MMA as the model system.

The kinetics of monomer radical formation in sonochemical polymerization depends on concentration of monomer molecules and (instantaneous) concentration of the radicals generated from cavitation bubble collapse. We use the word “instantaneous”, as the radicals are extremely unstable entities and they react immediately after being released into the medium with cavitation bubble collapse, without diffusing away from the location of bubble collapse. Therefore, the rate of formation of monomer radicals (in other words, the “helpful” utilization of cavitation radicals towards formation of monomer radicals) also depends on probability of interaction between the monomer molecules and radicals. If the concentration of radicals is very high, the droplets are likely to be “spot polymerized” by set of radicals inducing and terminating polymerization reaction [17,18]. In addition, as noted earlier, radial motion of cavitation bubble also gives rise to emulsification due to convection created in the medium due to microturbulence and shock waves.

In this study, we try to assess the relative influence of the physical effect (emulsification) and chemical effect (radical generation) of the cavitation bubbles on the outcome of copolymerization process, i.e. molar ratio of two monomers in the copolymer, and molecular weight and polydispersity of the copolymer. We choose three experimental parameters for the assessment, viz. presence or absence of external initiator, ratio of monomers in the reaction mixture and use of sparge gases (argon and nitrogen) during sonication. The rationale underlying choice of these parameters will be explained in subsequent sections. The mathematical model used in this study can quantitatively predict the amount of radical generation and the magnitudes of microturbulence and shock waves generated by single cavitation bubble of either argon or nitrogen.

2. Experimental

2.1. Experimental setup

The reactions were carried out in a jacketed reactor made of borosilicate glass (a schematic of the setup has been given in our previous paper [40]). The dimensions of the reactors were: height = 120 mm, diameter = 50 mm, inner diameter of jacket = 62 mm and glass thickness = 2 mm. In order to avoid rise in temperature of the reaction mixture during sonication (as the polymerization progresses), cooling water was circulated in the reactor jacket. The sonication of the reaction mixtures was accomplished by a microprocessor based and programmable ultrasonic processor (Sonics and Materials Inc., Model VCX 500). This processor had a frequency of 20 kHz with maximum power output of 500 W. The processor has variable power output control, which was set at 20% during experiments, resulting in net consumption of 100 W power during sonication. It needs to be mentioned that this value corresponds to the theoretical maximum ultrasound intensity. The actual ultrasound intensity in the medium was calibrated using calorimetry [41]. For a theoretical intensity of 100 W, the sonicator probe produced an ultrasound wave with pressure amplitude of 1.5 bar (for greater details on calorimetric determination of ultrasound intensity in the medium and pressure amplitude of ultrasound wave, please refer to Appendix A). Ultrasound pressure amplitude of 1.5 bar corresponds to the actual ultrasound intensity (delivered to the medium) of 0.8 W/cm^2. In addition the processor was equipped with facility of automatic amplitude compensation, due to which the power delivered to the medium stays constant during experiments. The sonicator probe of this processor was made of special titanium alloy and had a tip diameter of 13 mm. The time of the sonication could also be precisely controlled through the processor.

2.2. Experimental procedure

Synthesis grade monomers, viz. MMA and BA, were procured from Loba–Chemie. Prior to polymerization, the inhibitor in the monomers was removed by passing them through column of neutral alumina. The mesh size of the neutral alumina was 70–230 mesh. The two monomers were mixed in required proportions before transferring to the reactor. In any typical experiment, the reaction mixture comprised of monomers (7.5 g total), ammonium persulfate (0.4 g) as the initiator, surfactant SDS (0.5 g), and water (67.5 g, Millipore, Elix 3) as the bulk medium for emulsion. Exact composition of the reaction mixtures in various experiments is given in Table 1. The surface tension of water after addition of surfactant (below CMC level) was measured using a tensiometer (Make: Kruus; Model: K9–Mk1) with Dunoy ring method as 0.057 N m^{-1}. Other properties of water such as viscosity, density and vapor pressure, however, remain practically unaffected with addition of SDS. Two gases, viz. argon and nitrogen, were used for purging the reaction mixture. Prior to sonication, the reaction

Table 1
Composition of the reaction mixture in different experiments.

Weight ratio of monomers $(M_1/M_2)_w$	Actual quantity of monomer added (g)		Molar ratio of monomers $(M_1/M_2)_m$
	M_1	M_2	
Experiments with sparging of argon			
1:4	1.5	6	0.32
2:3	3	4.5	0.85
4:1	6	1.5	5.12
Experiments with sparging of nitrogen			
1:4	1.5	6	0.32
2:3	3	4.5	0.85
4:1	6	1.5	5.12

M_1 – Monomer 1 (MMA or MMA); M_2 – Monomer 2 (BA).
In addition to the above, reaction mixture in each experiment comprised of 67.5 mL water (as solvent), 0.5 g SDS (as surfactant) and 0.4 g ammonium persulfate (as initiator). Experiments were also conducted with above reaction mixtures except addition of the external initiator.

mixture was purged with required gas for 45 min so as to remove dissolved oxygen. Thereafter, the gas stream was removed from the emulsion and was passed over the surface of the liquid mixture. Sparging of the reaction mixture with either argon or nitrogen leaves a large number of suspended bubbles of the gas in the medium, which could form nuclei for cavitation events. The radial motions of cavitation bubbles of argon and nitrogen have different character. The cavitation intensity (i.e. temperature and pressure peak reached in the bubble at the transient collapse) generated by the bubbles of argon (a monatomic gas) is much higher than nitrogen, which is a diatomic gas.

The polymerization reaction was initiated by subjecting the reaction mixture to cycles of continuous sonication for 10 min, with 5 min pauses between sonication periods. Initial temperature of reaction mixture was 25 °C. Due to periodic sonication cycle and the immersion of the reaction vessel in an ice/water bath, the variation in temperature of the reaction mixture during sonication was ±5 °C.

In addition to these experiments, we have conducted two supplementary experiments as follows: (1) Experiment with ultrasound irradiation of the reaction mixture without addition of the external initiator (with other composition of reaction mixture remaining the same); (2) Experiment with addition of initiator to reaction mixture, which was agitated (250 rpm) using a magnetic stirrer at room temperature. As explained in the subsequent sections, the first supplementary experiment was aimed at assessing the role of radicals generated from cavitation bubbles (i.e. the chemical effect of cavitation) on the polymerization process, while the second supplementary experiment was aimed at assessing the physical effect of cavitation bubbles.

After completion of 60 min of sonication, the polymerization was terminated with addition of a pinch of hydroquinone to reaction mixture. A small aliquot (~5 mL) of the reaction mixture was taken out for the determination of conversion of monomers. Small coagulum of polymer attached to the tip of the sonicator probe was carefully removed with a spatula, and was mixed with reaction mixture. The reaction mixture was left for cooling thereafter in the refrigerator for at least 24 h. Next, the latex samples were dried. In order to remove the surfactant, the dried latex samples were dissolved in THF and precipitated by addition of water. The precipitated samples were again dried and weighed. The conversion of the monomers achieved during 60 min of sonication was determined using a simple method described by Bradley and Grieser [12] (for greater details on this refer to Appendix A). All experiments were conducted in duplicate to ensure reproducibility of the results.

2.3. Analysis of the polymerization product

The dried latex samples were analyzed with NMR to determine the copolymer composition and with Gel Permeation Chromatograph (GPC) to determine molecular weight of copolymer formed. More details of these techniques are as follows:

NMR Analysis: NMR spectra of the copolymer latex samples were obtained using Varian 400 MHz FTNMR spectrometer with integrator using 20 mg of copolymer samples dissolved in 1 mL of $CDCl_3$. From the NMR spectra of copolymer MMA–BA, the peak due to the $-O-CH_3$ protons in (MMA) was resolved from $-O-CH_2-$ in (BA). The monomer compositions of the copolymers were calculated from the ratios of the areas under those peaks as measured by the integral curves, the areas being proportional to the number of protons contributing to the peaks [42].

$\int -OCH_2- \propto 2$ (number of BA units in chain)
$\int -OCH_3 \propto 3$ (number of MMA units in chain)

in which $\int -OCH_2$ and $\int -OCH_3$ are integrals of $-O-CH_2-$ and $-O-CH_3$ peaks respectively. If X is the molar ratio MMA/BA in copolymer, then: $\int -OCH_2-/\int -OCH_3 = 2/(3X)$

Molecular weight analysis: The GPC analysis was performed on Waters 2410 instrument with ultrastyragel 100 Å 7.8 × 300 mm waters column employing polystyrene as internal standard and THF as effluent.

Determination of reactivity ratios: The conventional first-order Markov or termination model of copolymerization gives the relation between monomer ratio in the reaction mixture ($[M_1]/[M_2]$), ratio of two monomer units in copolymer ($d[M_1]/d[M_2]$) and the reactivities of two monomers (r_1 and r_2) as follows [43]:

$$\frac{d[M_1]}{d[M_2]} = \frac{[M_1]}{[M_2]} \frac{(r_1[M_1] + [M_2])}{([M_1] + r_2[M_2])} \quad (1)$$

The above equation assumes that the reactivity ratio of the propagating species is dependent only on the monomer unit at the end of the chain. Fineman and Roos [44] rearranged above equation as:

$$G = r_1 F - r_2 \quad (2)$$

where $G = X(Y-1)/Y$, $F = X^2/Y$, $X = [M_1]/[M_2]$ and $Y = d[M_1]/d[M_2]$. Plot of variable G against F yields a straight line with slope r_1 and intercept r_2. For our analysis we ascribe subscript 1 to MMA and subscript 2 to BA.

3. Mathematical model for cavitation bubble dynamics

Ultrasound manifests its physical and chemical effects through phenomenon of cavitation. Passage of ultrasound through liquid creates sinusoidal variation in the bulk pressure. Cavitation essentially means nucleation, growth and transient collapse of small gas bubbles (in the size range of few microns) under the influence of time variant bulk pressure in the liquid. The nuclei for cavitation phenomena are small air pockets trapped in the solid boundaries in the medium such as the walls of the reactor or the surface of the sonicator probe [45].

3.1. Limitations of the mathematical models

The approach of mathematical modeling for estimation of the physical and chemical effect of cavitation also has certain limitations, which we outline here. All of the chemical systems in practice are essentially *multibubble systems* where the gross physical and chemical effect is a result of collective oscillations and collapse of millions of cavitation bubbles. It is estimated that water under normal conditions could have bubble population in the range 10^5–10^7 per cm^3 [46]. With such large population of cavitation bubbles, it is rather obvious that strong interaction would exist among them. Although a few authors have attempted to model multibubble systems [47], a rigorous mathematical model that takes into account the *entire* physics of the multibubble system (including other physical phenomena such as bubble–bubble coalescence, clustering and rectified diffusion, which slow accumulation or dissolution of gas in the cavitation bubble) has not been developed so far. Moreover, an accurate estimation of the bubble population in the medium is also extremely difficult.

Single bubble models, however, can qualitatively describe all characteristic (both physical and chemical) features of multibubble systems, as demonstrated by many previous authors [41,48–51]. We believe that single bubble model is sufficient in the context of the present study where we try to form link between the physics and chemistry of the sonochemical emulsion polymerization system.

Table 2(A)
Summarization of the bubble dynamics formulation.

Variable	Equation	Initial values
1a. Radius of the bubble (R) 1b. Bubble wall velocity (dR/dt)	*Equation* 1[a]: $\left(1-\frac{dR/dt}{c}\right)R\frac{d^2R}{dt^2}+\frac{3}{2}\left(1-\frac{dR/dt}{3c}\right)\left(\frac{dR}{dt}\right)^2=\frac{1}{\rho_L}\left(1+\frac{dR/dt}{c}\right)\left(P_i-P_t\right)+\frac{R}{\rho_L c}\frac{dP_i}{dt}-4\nu\frac{dR/dt}{R}-\frac{2\sigma}{\rho_L R}$ *Other parameters*: Internal pressure in the bubble: $P_i=\frac{N_{tot}(t)\,kT}{[4\pi(R^3(t)-h^3)/3]}$ Pressure in bulk liquid medium: $P_t=P_0-P_A\sin(2\pi ft)$	At $t=0$, $R=R_o$ and $dR/dt=0$.
2. Number of water molecules in the bubble (N_w)	*Equation* 2: $\frac{dN_w}{dt}=4\pi R^2 D_w\frac{\partial C_w}{\partial r}\Big\vert_{r=R}\approx 4\pi R^2 D_w\left(\frac{C_{wR}-C_w}{l_{diff}}\right)$ *Other parameters*: Instantaneous diffusive penetration depth: $l_{diff}=\min(\sqrt{RD_w/\vert dR/dt\vert},\ R/\pi)$	At $t=0$, $N_w=0$
3. Heat transfer through bubble (Q)	*Equation* 3: $\frac{dQ}{dt}=4\pi R^2\lambda\frac{\partial T}{\partial r}\vert_{r=R}\approx 4\pi R^2\lambda(\frac{T_0-T}{l_{th}})$ *Other parameters*: Thermal diffusion length: $l_{th}=\min(\sqrt{R\kappa/\vert dR/dt\vert},\ R/\pi)$	At $t=0$, $Q=0$
4. Temperature of the bubble (T)	*Equation* 4: $C_{V,mix}dT/dt=dQ/dt-P_i dV/dt+(h_w-U_w)dN_w/dt$ *Other parameters*: Mixture heat capacity: $C_{V,mix}=\sum C_{V,i}N_i$ Molecular properties of water: Enthalpy: $h_w=4kT_o$ Internal energy: $U_w=N_w kT\left(3+\sum_{i=1}^{3}\frac{\theta_i/T}{\exp(\theta_i/T)-1}\right)$ Heat capacity (Ar): $C_V=3kN_{Ar}/2$ Heat capacity of other species ($i=N_2/H_2O$): $C_{V,i}=N_i k(f_i/2+\sum\left(\left(\theta_i/T\right)^2\exp(\theta_i/T)/(\exp(\theta_i/T)-1)^2\right))$	At $t=0$, $T=T_o$

R – radius of the bubble; dR/dt – bubble wall velocity; c – velocity of sound in bulk liquid medium; ρ_L – density of the liquid; ν – kinematic viscosity of liquid; σ – surface tension of liquid; λ – thermal conductivity of bubble contents; κ – thermal diffusivity of bubble contents; θ – characteristic vibrational temperature(s) of the species; N_w – number of water molecules in the bubble; t – time, D_w – diffusion coefficient of water vapor; C_w – concentration of water molecules in the bubble; C_{wR} – concentration of water molecules at the bubble wall or gas–liquid interface; Q – heat conducted across bubble wall; T – temperature of the bubble contents; T_o – ambient (or bulk liquid medium) temperature; k – Bolzmann constant; N_{Ar} – number of Ar molecules in the bubble; f_i – translational and rotational degrees of freedom; $C_{V,i}$ – heat capacity at constant volume; N_{tot} – total number of molecules (gas + vapor) in the bubble; h – van der Waal's hard core radius; P_o – ambient (bulk) pressure in liquid; P_A – pressure amplitude of ultrasound wave; f – frequency of ultrasound wave.

[a] Equation (1) can be split into two simultaneous equations by a simple substitution: $dR/dt=s$.

3.2. Diffusion limited model

Modeling of the radical generation by cavitation bubbles is an active area of research for past two decades and various authors have addressed the matter with different approaches [36–38,46,52–57].

For our purpose, we use the diffusion limited model of Toegel et al. [57], which has been described extensively in previous papers from our group [40,41,51,58]. Hence, we describe herewith only main features of the model. Essential equations and thermodynamic data of this model have been summarized in Tables 2(A) and (B). For greater details, the reader is referred to the papers mentioned above as well as the original paper [57]. The main components of the model (consisting of set of 4 simultaneous ordinary differential equations as initial value problem) are follows:

(1) Keller–Miksis equation for the radial motion of the bubble [59–61].
(2) Equation for the diffusive flux of water vapor and heat conduction through bubble wall. The transport parameters for the heat and mass transfer (thermal conductivity and diffusion coefficient) are determined using Chapman–Enskog theory using Lennard–Jones 12–6 potential at the bulk temperature of the liquid medium [62–65]. Thermal and diffusive penetration depths are estimated using dimensional analysis.
(3) Overall energy balance treating the cavitation bubble as an open system.

The monomers added to water have finite solubility. Thus, these monomers (or solutes in water) can also evaporate into the bubble during the expansion phase of radial motion of bubble. However, for reasons stated later in this section, we have ignored this evaporation. This model also ignores the diffusion of gases across the bubble wall as the time scale for the diffusion of gases is much higher than the time scale for the radial motion of bubble. From the numerical solution of bubble dynamics model that gives time history of bubble radius (R), bubble wall velocity (dR/dt) and acceleration (d^2R/dt^2), the convection generated by the cavitation bubble can be estimated. In a homogeneous medium, the principal contribution to the convection is by microturbulence (oscillatory

Table 2(B)
Thermodynamic properties of various species.[a]

Species	Degrees of freedom (translational + rotational) (f_i)	Lennard–Jones force constants		Characteristic vibrational temperatures θ (K)
		σ (10^{-10} m)	ϵ/k (K)	
N_2	5	3.68	92	3350
H_2O	6	2.65	380	2295, 5255, 5400
Ar	3	3.42	124	–

[a] Data taken from [62,64,74].

Table 2(C)
Quantification of convection generated by cavitation bubble [32,33].

Parameter	Equation
1. Microturbulence	$V_{turb}(r,t)=\frac{R^2}{r^2}\left(\frac{dR}{dt}\right)$
2. Shock waves	$P_{AW}(r,t)=\frac{\rho}{4\pi r}\frac{d^2V_b}{dt^2}=\rho\frac{R}{r}\left[2\left(\frac{dR}{dt}\right)^2+R\frac{d^2R}{dt^2}\right]$

velocity field generated in the close vicinity of the bubble due to rapid motion of the bubble wall) and shock waves (wave generated in the bulk liquid due to sudden reflection of the fluid elements converging towards the bubble wall during radial motion, when the bubble wall comes to a sudden halt at the point of minimum compression). Table 2(C) describes formulae for these two phenomena. It could be inferred from these formulae that magnitudes of both shock waves and microturbulence vary inversely with *r*, i.e. the distance from the bubble wall [32,33,66]. Thus, the intensity of the convection induced by the cavitation bubble is rather "local", i.e. it is the highest in the close vicinity of the bubble, and diminishes very rapidly away from it.

3.3. Quantification of physical effect (convection) of cavitation bubble dynamics

The principal physical effect of cavitation bubble dynamics is generation of convection in the medium. However, this convection is of different kind. Various physical phenomena, such as microturbulence, shock waves and microjets, related to radial motion of cavitation bubble contribute to this convection. Each of these phenomena has a distinct character and they also differ widely in the magnitude.

3.4. Numerical solution

The set of four ODEs described in Table 2(A) can be solved simultaneously using Runge–Kutta adaptive step size method [67]. Simulations have been performed for two kinds of bubbles, viz. nitrogen and argon. The condition for bubble collapse is taken as the first compression after an initial expansion [38]. Four important parameters required for the simulation of bubble dynamics equation are frequency (f) and pressure amplitude (P_A) of ultrasound, partial pressures of solvent (P_w) and solutes (P_{BA} and P_{MMA}) at the bubble interface (on which the extent of evaporation of the solvent, i.e. water, and solutes, i.e. monomers, in the bubble depends) and the equilibrium bubble radius (R_o).

Frequency: The frequency of the ultrasound was taken as 20 kHz – same as the frequency of the ultrasound processor used in the experiments.

Pressure amplitude: As explained in Appendix A, the pressure amplitude of the ultrasound wave generated by the sonicator probe was determined calorimetrically as 1.5 bar [41]. The ultrasound wave generated at the sonicator probe tip undergoes attenuation as it propagates through the medium. The attenuation is due to viscous and thermal dissipation and scattering/absorption of sound waves due to bubbles [68]. For exact estimation or measurement of the local pressure amplitude (at any point in the reaction mixture away from sonicator probe tip), very small dimension or needle kind of hydrophones are needed, which were not available with us. With this limitation, we have assumed a *typical or representative* value for attenuation of the sound wave as 15%. The average amplitude of the ultrasound wave prevalent in the reaction mixture, is thus, $P_A \approx 1.25$ bar, and this value has been used in the numerical simulations. With extensive simulations of the bubble dynamics model (not included in this manuscript), we have ascertained that any other choice of value for P_A (for example 1.3 bar or 1.2 bar etc.) makes only minor quantitative changes to the simulations results. These values do not alter the trends observed in simulation results.

Equilibrium bubble radius: The equilibrium radius of the bubbles is difficult to estimate. Moreover, it continuously keeps on changing due to various phenomena such as clustering and fragmentation of bubbles during radial motion and rectified diffusion [69,70]. Therefore, in bubble dynamics formulations, this quantity is used as a parameter. We have set the equilibrium size of bubbles at 10 μm for simulation as a representative value.

Evaporation of the solvent and solutes in the bubble: The liquid medium in the present study comprises of water with two solutes (viz. the BA and MMA monomers) dissolved in it. All of these evaporate and diffuse into the bubble. However, the extent of evaporation depends on the partial pressure of these components at the bubble wall. The diffusion of these molecules depends on the driving force, which is the difference in the partial pressure at the bubble wall and at the bubble core. We qualitatively assess the extent of evaporation of each of the components. The vapor pressure of water ($P_{v,w}$), methyl methacrylate ($P_{v,MMA}$) and butyl acrylate ($P_{v,BA}$) (in pure form)is given by following Antoine type expressions:

$$P_{v,w} = \frac{10^5}{760}\exp\left(18.3036 - \frac{3816.44}{T - 46.13}\right) \quad (3)$$

$$P_{v,BA} = 10^5 \times 10^{(4.42683 - 1658.03/(T - 45.561))} \quad (4)$$

$$P_{v,MMA} = 10^5 \times 10^{(4.34032 - 1299.069/(T - 46.183))} \quad (5)$$

As mentioned in Experimental section, the temperature of the reaction mixture was 25 ± 5 °C during experiments. As a conservative estimate, we assume $T = 30$ °C (or 303.16 K) for calculation of vapor pressure of each of the components as: $P_{v,w} = 4167$ Pa; $P_{v,BA} = 978$ Pa and $P_{v,MMA} = 6250$ Pa. We now need to calculate the partial pressure.

The solubilities of the two monomers are as follows: BA = 0.002 g mL^{-1} and MMA = 0.015 g mL^{-1}. As stated in Experimental section, the total reaction mixture comprised of 67.5 mL water and a total of 7.5 g of monomers in certain proportions (1:4, 2:3 and 4:1). As both monomers are sparingly soluble in water, we assume that solubility of one monomer is not affected in presence of other. Thus, in 67.5 mL water, the total solubility of each monomer is: BA = 0.135 g and MMA = 1.0125 g. The quantity of each monomer added to water in any of the experiment is more than these values (refer to Table 1 for composition of reaction mixtures). Thus, it is reasonable to assume that water is saturated with the monomers in each experiment. With this, the total mole fraction of each of the component in the reaction mixture can be easily determined as follows:

(1) Water = 67.5 g or 3.75 gmoles. Mole fraction (x_w) = 0.99703
(2) MMA = 1.0125 g or 0.01011 gmoles. Mole fraction (x_{MMA}) = 2.688×10^{-3}
(3) BA = 0.135 g or 0.0010533 gmoles. Mole fraction (x_{BA}) = 2.8×10^{-4}

Once again, on the basis that both monomers are sparingly soluble in water, the partial pressures of each component could be calculated by product of the mole fraction of the component and its vapor pressure in pure form. Thus, the partial pressures are:

(1) Water: $P_w = x_w \times P_{v,w} = 0.99703 \times 4167 = 4155$ Pa
(2) BA: $P_{BA} = x_{BA} \times P_{v,BA} = 2.8 \times 10^{-4} \times 978 = 0.2738$ Pa
(3) MMA: $P_{MMA} = x_{MMA} \times P_{v,MMA} = 2.688 \times 10^{-3} \times 6250 = 16.8$ Pa

On the basis of the partial pressures of various components at the bubble interface, it can be perceived that extent of evaporation of water will be far higher (at least 2 to 3 orders of magnitude) than that of any of the two monomers. The bubble contents at any time during the radial motion will thus be dominated by the water vapor. The peak temperature reached during transient collapse will also be determined by the water vapor content of the bubble. For these reasons, we have ignored the evaporation of monomer molecules

into the bubble during its radial motion. While calculating the composition of the bubble at the time of collapse, we assume that thermodynamic equilibrium is attained. This assumption is based on the relative magnitudes of bubble collapse time scale ($\sim 10^{-8}$ s [38]) and time scale of various radical reactions ($\sim 10^{-10}$ s [51]). The equilibrium composition of the bubble contents at the conditions of transient collapse was calculated using software FACTSAGE, which uses the free-energy minimization algorithm proposed by Eriksson [71].

4. Results and discussion

A sonochemical system has complex mechanism with physics and chemistry strongly interwoven. The principal physical effect of ultrasound is cavitation, which causes energy concentration that has several physical and chemical manifestations. Both of these could possibly affect the net outcome of copolymerization process. Our attempt in this study is to explore the physical mechanism of the sonochemical emulsion copolymerization of the process. An important parameter in copolymerization process that affects the yield and composition of the copolymer is reactivity ratio of the monomers. This parameter determines the type of copolymerization behavior. Ideal copolymerization occurs when the product of reactivity ratio of the two monomers (denoted as r_1 and r_2) is unity. In this case the propagating species (with any of the monomer unit at the end of the chain) shows same preference for adding any of the two monomers. Moreover, if $r_1 = r_2 = 1$, the two monomers have equal reactivities towards propagating species with either M_1 (monomer 1) or M_2 (monomer 2) at the terminal end, and the copolymer composition is same as the monomer feed in the reaction mixture with random placement of two monomers along copolymer chain. When the reactivities of the two monomers are different ($r_1 > 1$ & $r_2 < 1$ or $r_1 < 1$ & $r_2 > 1$), one of the monomers is more reactive than the other towards propagating species and the resulting copolymer is richer with more reactive monomer with random placement. When neither r_1 nor r_2 is greater than 1, alternating copolymerization occurs. Under ideal case, when $r_1 = r_2 = 0$, extreme alternating behavior results and copolymer comprises of two monomer units in equimolar amounts in non-random, alternating arrangement. In this situation the ratio of two monomer units in copolymer is 1 for all feed compositions of monomers. Under practical situation, moderate alternating behavior is seen when both r_1 and r_2 are very small (yet non-zero), and the product $r_{1r_2} \ll 1$. For such a case, the copolymerization composition tends towards alternation but not perfectly. If $r_1 > r_2$, the copolymer still contains greater fraction of first monomer, as the propagating species preferentially adds the first monomer. The most important (and advantageous) consequence of $r_1, r_2 < 1$ is that large range of feed compositions yield copolymers containing sizeable amount of both monomers.

With this preamble, we first present the experimental results followed by results of simulations of cavitation bubble dynamics. Later, we try to correlate the two, and try to establish link between the cavitation physics and polymer chemistry.

4.1. Experimental results

As noted in Section 2, experiments were done in two categories, viz. with and without addition of the external initiator (ammonium persulfate). No reaction occurred in absence of external initiator. Similarly, no polymerization was seen at room temperature in the mechanically stirred reaction mixture with externally added initiator.

For the experiments with ultrasound irradiation using reaction mixtures with externally added initiator, representative NMR spectra of copolymers obtained in experiments with argon-sparged and nitrogen-sparged reaction mixtures are depicted in Figs. 1 and 2, respectively. The plot of equation (1) (variable G against F) for determination of the reactivity ratios of the two monomers is given in Fig. 3. The compositions of copolymers for argon and nitrogen sparged reaction mixtures along with the reactivities of the two monomers are given in Table 3(A), while the summary of the GPC characterization (i.e. weight and chain-average molecular weights of the copolymers and the polydispersity of the copolymers) is given in Table 3(B). Also given in Table 3(A) are the theoretical values of copolymer composition (calculated using Equation (1)) using the reactivity ratios determined with Equation (2). From these results, we identify three peculiar features of copolymer composition:

1. Overall conversion of monomers in 60 min of sonication is same for argon as well as nitrogen sparged mixtures for any given ratio of monomers in the reaction mixture.
2. For monomer weight ratios (MMA:BA) of 1:4 and 2:3, the molar composition of MMA in copolymer (0.81 and 1.3 respectively for argon sparged solutions and 0.61 and 1.34 respectively for nitrogen sparged solutions) is much higher than in the reaction mixture as monomer (0.32 and 0.85 respectively for weight of 1:4 and 2:3).
3. For monomer weight ratio of 4:1 (MMA:BA), however, the molar composition of MMA in copolymer (2.5 for argon sparged solution and 2.42 for nitrogen sparged solution) is lower than that in reaction mixture (5.12). Nonetheless, the copolymer is still dominated by MMA, as indicated by molar compositions of MMA in copolymer greater than 1.
4. The sparge gas has only marginal to negligible effect on copolymer composition. Essentially same composition of copolymer (in terms of MMA:BA molar ratio) is seen for all compositions of the reaction mixtures (in terms of weight ratio of the monomers) for both argon and nitrogen sparged solutions.
5. The polydispersity of the copolymer is 1, which essentially indicates uniform polymerization (i.e. all polymer change have essentially same length). The reactivity ratio of MMA as well as BA is less than 1 for both argon and nitrogen sparged reaction mixtures. The theoretically calculated and experimentally determined copolymer compositions match reasonably well (±10–15%).

4.2. Simulation results

Fig. 4 depicts representative simulation of the radical motion of 10 micron nitrogen bubble. The summary of entire simulations is given in Table 4. From these results, we identify the following characteristic features:

1. The cavitation intensity of an argon bubble, indicated by the temperature peak attended at the transient collapse, is much higher than nitrogen bubble. The temperature peak (T_{max}) for argon bubble is 3922 K while that for nitrogen bubble is 2476 K.
2. Consequently, the total production of various radicals (H•, •OH, $HO_2^{\bullet}$ and $O^{\bullet}$) per bubble for argon (3.4485×10^9 radicals) is also higher than nitrogen (6.7419×10^7 radicals).
3. Although the microturbulence velocities from the two types of bubble are similar (viz. 6.039 mm s^{-1} for argon and 7.066 mm s^{-1} for nitrogen), the magnitude of the shock wave generated by nitrogen bubble (2.5 bar) is somewhat higher than argon bubble (1.4 bar).
4. The temperature peaks at transient collapse seen for both bubbles are lesser than those reported in literature (5000 K [39,72]). We attribute this to lower surface tension of water due to addition of SDS.

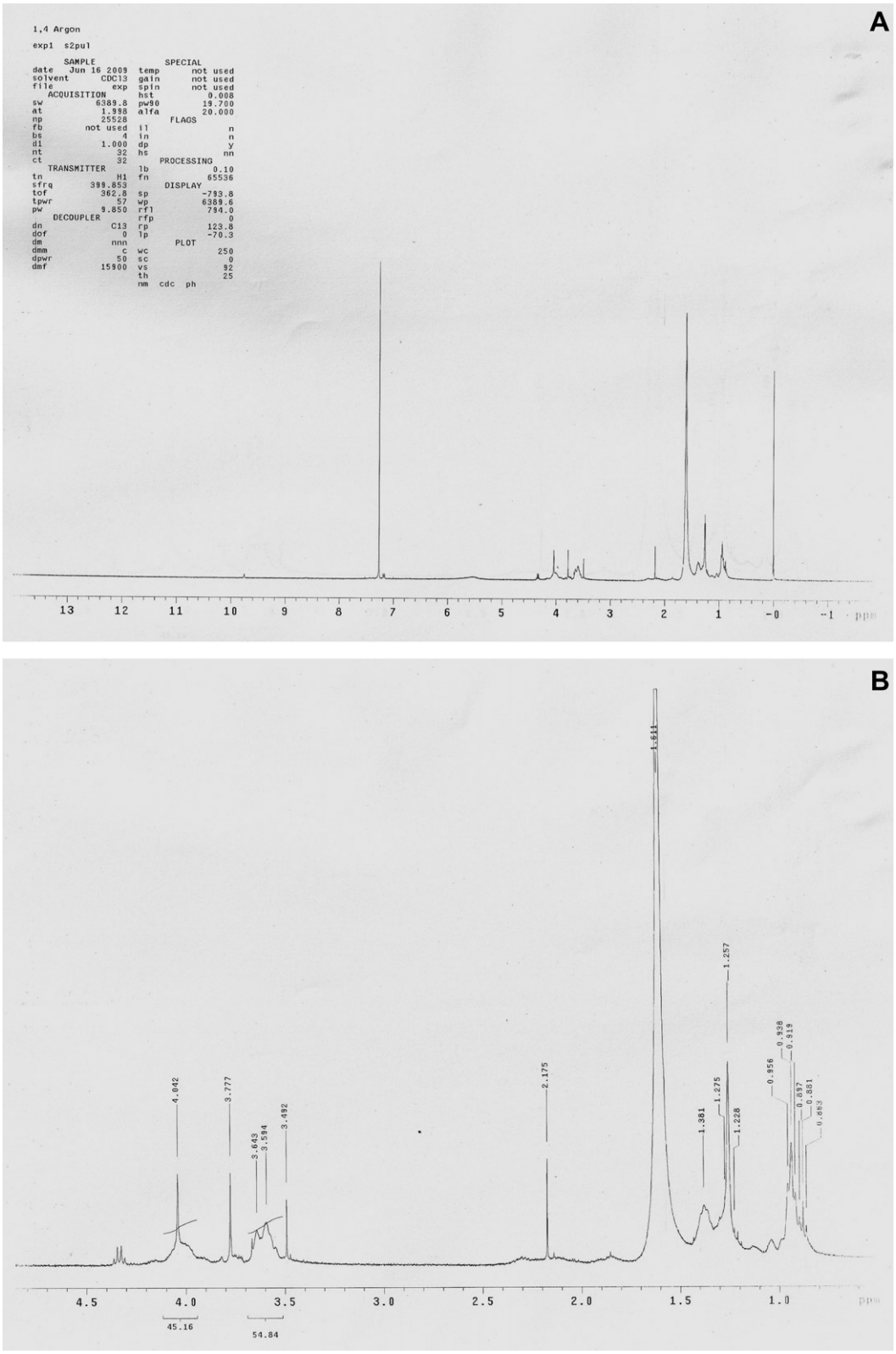

Fig. 1. NMR analysis of polymer samples synthesized with monomer ratio of 1:4 and argon sparging. (A) Complete spectrum; (B) Resolved spectrum for the $-O-CH_2-$ ($\delta = 4.1$) and $-O-CH_3-$ ($\delta = 3.6$) peaks.

4.3. Analysis

We now try to correlate the experimental and simulation results to deduce the exact nature of influence of ultrasound on the copolymerization system. However, prior to the main analysis, we would like to point out a basic difference in the nature of polymerization of BA and MMA molecules. The termination of BA radical occurs by combination reaction:

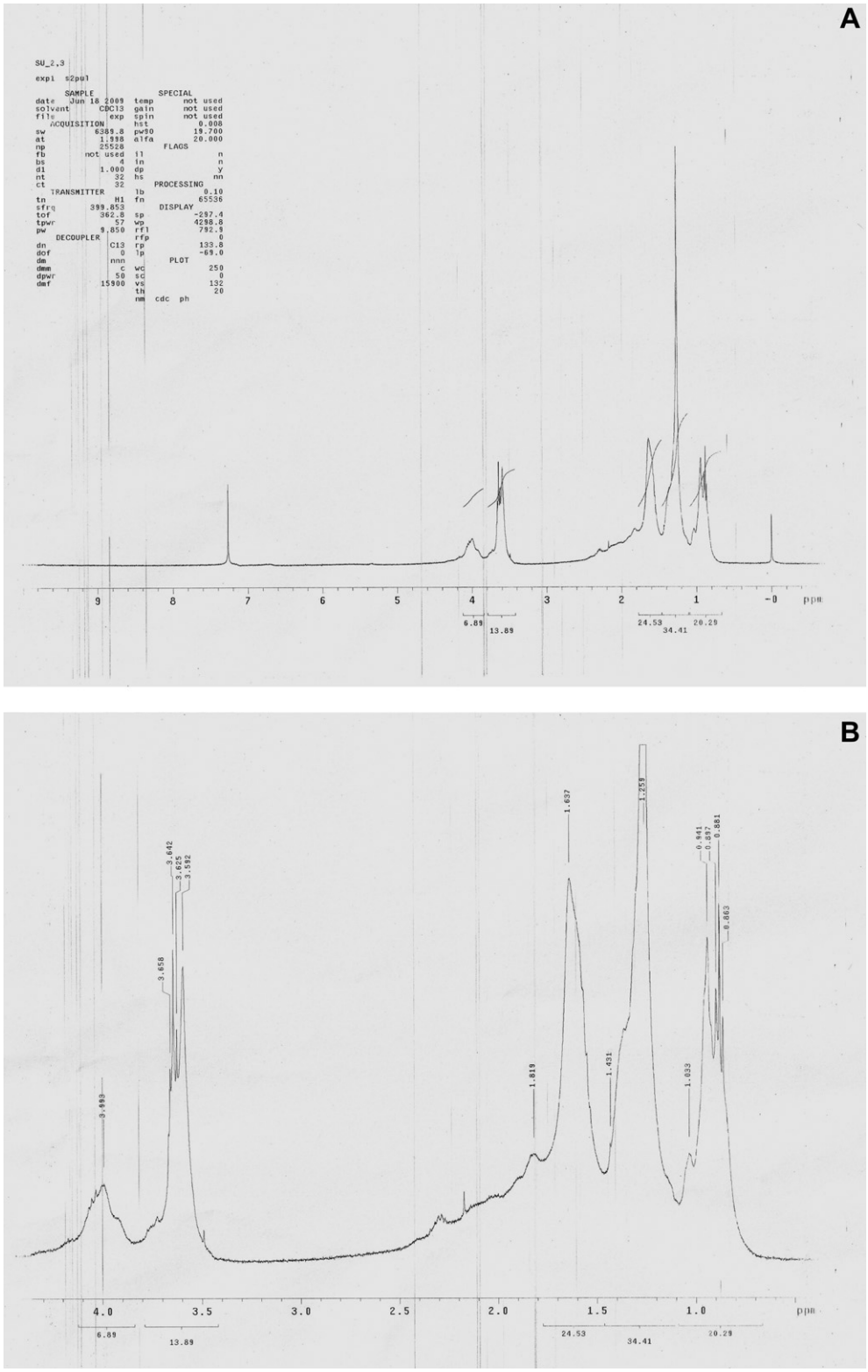

Fig. 2. NMR analysis of polymer samples synthesized with monomer ratio of 2:3 and nitrogen sparging. (A) Complete spectrum; (B) Resolved spectrum for the $-O-CH_2-$ ($\delta = 4.1$) and $-O-CH_3-$ ($\delta = 3.6$) peaks.

$$-M^{\bullet}_{BA,i} + -M^{\bullet}_{BA,i} \rightarrow M_{BA,i+j}$$

while, termination of the MMA radical occurs by disproportionation with generation of an unsaturated and a saturated monomer molecule.

$$-M^{\bullet}_{BA,i} + -M^{\bullet}_{MMA,j} \rightarrow -M_{MMA,i} = + -M_{MMA,j}$$

The saturated monomer molecule can further react with initiator radical to generate MMA radical:

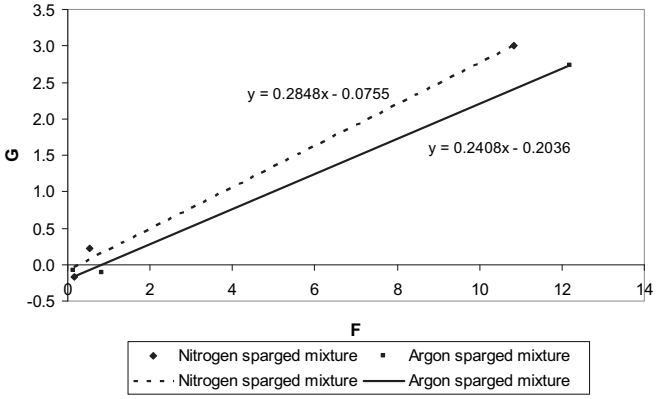

Fig. 3. Plot of Eq. (1) (variable G against F) for determination of reactivities of two monomers. The slope of the regression line gives r_{MMA} while the y-intercept gives r_{BA}.

$$-M_{MMA,j} + R^{\bullet} \rightarrow -M^{\bullet}_{MMA,j}$$

where $R^{\bullet}$ is the radical generated either from decomposition of the external initiator or radicals generated through dissociation of solvent molecules inside the bubble at the extreme conditions reached during transient collapse of cavitation bubbles.

- The preliminary reaction prior to commencement of polymerization is formation of monomer radicals from monomer molecules ($-M$):

$$-M + R^{\bullet} \rightarrow -M^{\bullet}$$

Depending on the number of monomer molecules and number of radicals, the limiting reactant is determined. If population of $-M$ molecules is much higher than $R^{\bullet}$, the limiting reactant are the radicals. For monomer (MMA:BA) weight ratio of 1:4 and 2:3, the population of BA molecules is higher than MMA, while for weight ratio of 4:1, population of MMA molecules dominate.

- No polymerization reaction seen in absence of external initiator indicates no role of radicals generated from cavitation bubbles (or the chemical effect of cavitation) in the polymerization process. This conclusion is further corroborated by the observation that copolymer composition obtained for argon and nitrogen sparge gases is essentially the same; although the extent of radical production by argon and nitrogen bubbles differs widely. This essentially indicates that radicals generated from cavitation bubbles are not utilized for polymerization due to mass transfer limitations (mentioned in Section 1.1). It is likely that these radicals simply recombine after being released into the bulk medium. With this, the principle role of ultrasound and cavitation in the copolymerization is physical one, i.e. formation of fine emulsion of monomer and water.
- No polymerization seen in the experiment at room temperature with addition of initiator in a mechanically stirred reaction mixture is a consequence of the fact that no thermal decomposition of the initiator occurred at room temperature, which would generate the radicals that would initiate polymerization.
- In presence of externally added initiator and ultrasound irradiation, the polymerization reaction occurred at room temperature. This result is dissimilar to conventional polymerization process in which the reaction mixture needs to be heated for dissociation of initiator to generate radicals for initiation of polymerization. We would attribute this discrepancy to the decomposition of external initiator at the bubble–bulk interfacial region. It was noted in Section 1 that the bubble interior reaches upto 5000 K and 500 bar during the adiabatic transient collapse. At this moment, the thin shell of bulk liquid medium surrounding the bubble also gets heated to few hundred °C and several bars. If an external initiator is present in the medium, it can undergo thermal decomposition at the bubble interface, generating radicals that could initiate the polymerization reaction. It should be categorically mentioned that the condition of higher temperature and pressure (either inside or outside the bubble) are highly localized (for example the shell of liquid surrounding the bubble that gets heated during transient collapse is only a few microns thick). The bulk conditions in the liquid medium are still ambient (1 atm and 25–30 °C). Thus, the role of cavitation phenomenon in the copolymerization process is of physical nature. We would also like to mention that this result is rather contradictory to the results of our earlier study [40] with single monomer, in which polymerization was seen without external initiator. Comparing this result with those from other groups, we find that Landfester [73] has used ultrasound only for agitation with external initiator being added to polymerization mixture. On the contrary, Bradley et al. [19] have reported sonochemical copolymerization of BA and MMA without addition of an external initiator.
- The ratio of MMA:BA in copolymer is higher than in the reaction mixture (or in the monomer form) for weight ratios of 1:4 and 2:3. However, for 4:1 weight ratio, the ratio of MMA:BA in copolymer is lesser than in the reaction mixture. We explain this on the basis of differences in reactivity of monomers and the limiting reactant. As the radicals responsible for initiation and propagation of polymerization were generated from externally added initiator, and as the quantity of external initiator added to reaction was same in all experiments, it is reasonable to assume that amount of initiator radicals converting monomer molecules into a radical was constant in all experiments.

For the weight ratio of 1:4, 2:3 and 4:1, the actual amount of MMA monomer used in the reaction mixture was 1.5, 3 and 6 g respectively. This would correspond to 0.015, 0.03 and 0.06 g mol respectively. On the other hand, the actual amount of BA used in the

Table 3(A)
Composition of copolymers in various experiments and reactivity ratios of monomers.

MMA:BA weight ratio	Molar ratio of monomers (MMA:BA)	Molar composition of copolymer (MMA:BA) experimental	Molar composition of copolymer (MMA:BA) calculated	Total conversion	Reactivity ratios
Results for argon sparged solutions					
1:4	0.32	0.81	0.66	63%	$r_{MMA} = 0.2408$
2:3	0.85	1.3	0.97	85%	$r_{BA} = 0.2036$
4:1	5.12	2.5	2.15	82%	
Results for nitrogen sparged solutions					
1:4	0.32	0.61	0.88	58%	$r_{MMA} = 0.2848$
2:3	0.85	1.34	1.14	81%	$r_{BA} = 0.0755$
4:1	5.12	2.42	2.42	85%	

M_w – weight average molecular weight.

Table 3(B)
Results of molecular weight determination of copolymer by GPC.[a]

Weight ratio of monomers (MMA:BA)	M_w	M_n	Polydispersity (M_w/M_n)
1:4	24,495	24,479	1.00067
2:3	23,233	23,132	1.004395
4:1	16,975	15,514	1.094170

M_n – number average molecular weight.
[a] Results for argon sparged reaction mixture.

reaction mixture for the same weight ratios is 6, 4.5 and 1.5 g respectively, which corresponds to 0.0468, 0.0351 and 0.0117 g mol respectively. These moles multiplied by the Avogadro number would give the number of molecules of each monomer in the reaction mixture.

The amount of initiator, i.e. ammonium persulfate, added to the reaction mixture for all experiments was 0.4 g, which corresponds to 1.754×10^{-3} mol. Ammonium persulfate decomposes as follows to yield sulfate ion-radicals, which initiate the polymerization reaction:

$$(NH_4)_2S_2O_8 \rightleftharpoons 2NH_4^+ + S_2O_8^{2-}$$
$$S_2O_8^{2-} \rightarrow 2^{\bullet}OSO_3^-$$

Thus, per mole of ammonium persulfate, 2 mol of initiator radicals are generated. Thus, in all experiments the net amount of initiator radicals would be 3.508×10^{-3}, which is smaller than moles of any monomer for any weight ratio. Therefore, for the reaction between monomer molecules and initiator radicals to generate monomer radicals, it is the initiator radical which would be the limiting reactant. These initiator radicals are competitively consumed by molecules of both monomers. However, consumption of initiator radicals by MMA is higher due to its higher reactivity (propagation rate constant of 650 L mol^{-1} s^{-1}) than BA (propagation rate constant of 200 L mol^{-1} s^{-1}) [25]. As a result, the quantity of MMA monomer radicals in the reaction mixture that undergo polymerization is higher than BA monomer radicals. Thus, the copolymer is dominated by the MMA.

For the weight ratio of 1:4 and 2:3, the number of moles of monomer MMA in reaction mixture is smaller than BA. However, due to higher reactivity of MMA, the fraction of MMA monomer molecules ending up in copolymer is higher than that of BA monomer molecules. As a consequence, the molar ratio of MMA in copolymer is higher than in reaction mixture for the monomer weight ratio of 1:4 and 2:3. For the weight ratio of 4:1, however, the population of MMA monomer molecules is much higher than BA monomer molecules. Therefore, the fraction of MMA molecules that get converted to monomer radicals and undergo polymerization to end up in copolymer is relatively lesser than the fraction of BA monomer molecules that undergo polymerization. Therefore, the molar ratio of MMA in copolymer is smaller than in the reaction mixture. Nonetheless, the total number of MMA monomer units in the copolymer is still higher than the BA monomer units, and hence, the molar ratio of MMA:BA in the copolymer (2.52) is greater than 1. This indicates that the copolymer is dominated by MMA for all weight ratios of monomers in the reaction mixture.

- The molecular weight of the copolymer reduces as the fraction of MMA in the reaction mixture (or monomer form) increases. We attribute this to the nature of termination of MMA and BA radicals. As noted earlier, termination of the two BA monomer radicals occurs by process of combination, which results in the formation of a larger molecule with higher molecular weight. Moreover, the termination of a BA monomer radical by a MMA monomer radical also occurs by combination, which results in formation of higher molecular weight product. On the other hand, termination of two monomer radicals of MMA occurs by disproportionation

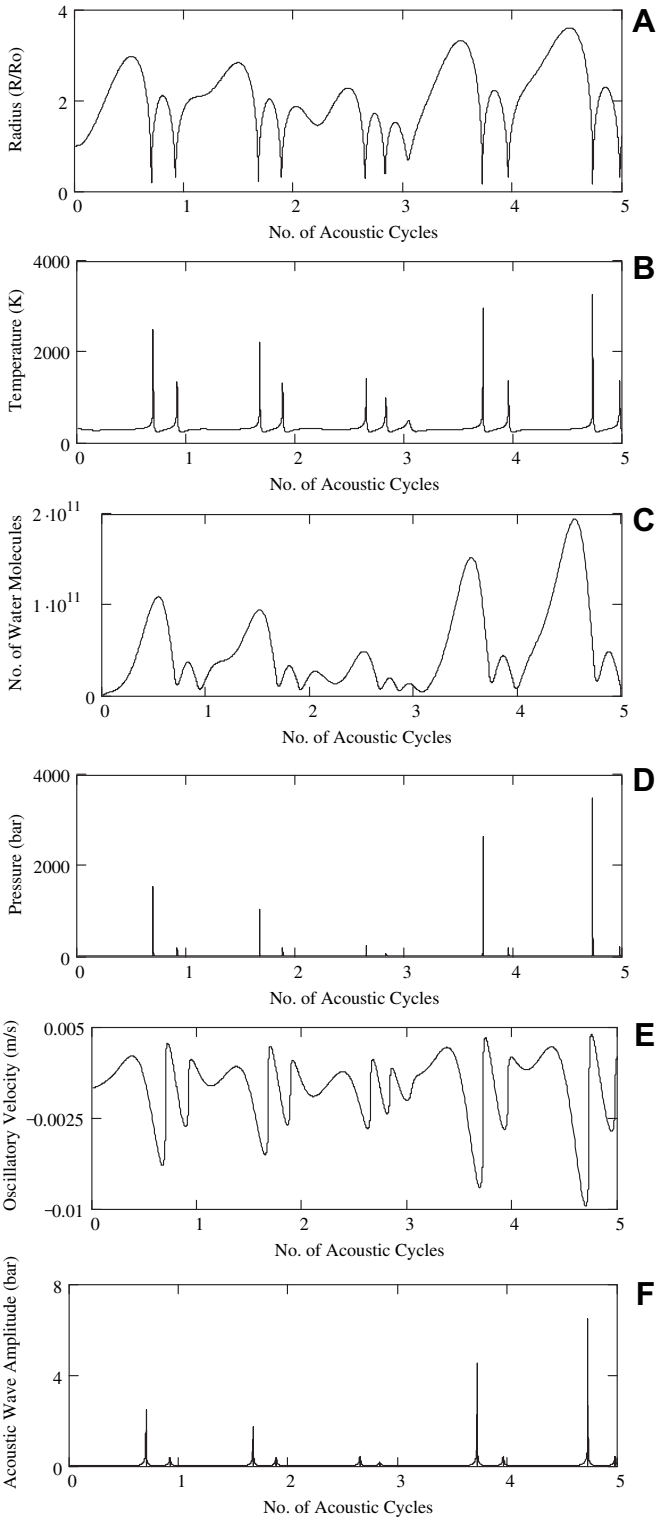

Fig. 4. Simulation results for radial motion of 10 micron nitrogen bubble. Time history of (A) normalized bubble radius (R/R_o); (B) temperature inside the bubble; (C) number of water molecules inside the bubble and (D) pressure inside the bubble. Simulation of radial motion of 10 micron nitrogen bubble. Convection generated in the medium due to (E) microturbulence and (F) shock or acoustic waves.

Table 4
Results of simulations of cavitation bubble dynamics.

Parameter	Bubble type	
	Argon	Nitrogen
(A) Conditions at transient collapse of the cavitation bubble		
T_{max} (K)	3922	2476
P_{max} (bar)	739.4	1531
N_w	2.04 E + 010	2.01 E + 010
V_{turb} (mm s^{-1})	6.039	7.066
P_{AW} (bar)	1.4	2.5
Species	Equilibrium composition (mole fraction)**	
	Argon bubble	Nitrogen bubble
(B) Equilibrium composition of the bubble contents at transient collapse		
H_2O	6.6491 E − 01	1.4587 E − 01
H_2	1.2955 E − 01	1.3826 E − 03
OH	1.1261 E − 01	4.6365 E − 04
H	3.7580 E − 02	2.1368 E − 05
O_2	3.6420 E − 02	2.0255 E − 04
O	1.8321 E − 02	4.6470 E − 06
HO_2	5.3602 E − 04	−
H_2O_2	7.0935 E − 05	−
N_2	−	8.5131 E − 01
NO	−	7.4693 E − 04
N_2O	−	1.5224 E − 06
Net yield of $O^{\bullet}$, $H^{\bullet}$, $HO_2^{\bullet}$ and $^{\bullet}OH$ radicals	3.4485 E + 09	6.7419 E + 07

** Species with equilibrium mole fraction less than 10^{-6} have been ignored.
T_{max} − temperature peak reached in the bubble at transient collapse; P_{max} − pressure peak reached in the bubble at transient collapse; N_w − number of water vapor molecules trapped in the bubble at transient first collapse; V_{turb} −microturbulence velocity generated by the cavitation bubbles (calculated as the average of the positive velocity, i.e. directed away from the bubble center and negative velocity, i.e. directed towards the bubble center); P_{AW} − pressure amplitude of the acoustic or shock wave emitted by the bubble.

that results in formation of saturated and an unsaturated monomer molecule. Thus, the net molecular weight of product remains unchanged, and such termination does not contribute to polymerization. The net outcome is that the rise in molecular weight is limited. The polydispersity of the copolymer is practically 1 for all monomer weight ratios, and thus, the polymerization is uniform.

- The most interesting result of our study is that the reactivities of both monomers (r_{MMA} and r_{BA}) are less than 1. This essentially means, per the preamble given earlier, that copolymerization process has alternating character. This result is in disagreement with earlier studies on sonochemical copolymerization of BA and MMA by Bradley et al. [19] and Bahattab et al. [25,26], which have reported r_{MMA} values of 2.55 and 3.66 respectively. The values of r_{BA} reported in these papers (0.36 by Bradley et al. [19] and 0.72 by Bahattab et al. [25,26]) are also higher than this study. We would like to ponder over possible causes leading to this effect. In the first place, the ultrasound intensity employed in this study (0.8 W/cm^2) is much smaller than used in earlier studies (7–9 W/cm^2). Therefore, the type of cavitation prevailing in the medium is of different kind. For low to moderate intensities (as used in this study), the cavitation is mostly gaseous type, i.e. the nuclei for cavitation are provided by the gas pockets trapped in the solid boundaries of the medium. On the other hand, for high ultrasound intensities as employed by Bradley et al. [19] and Bahattab et al. [25,26], vaporous cavitation (bubbles generated from local vaporization of liquid) also occurs in the medium. Radical generation from vaporous cavitation is much higher than gaseous one. Therefore, the net production of radicals in the medium in studies mentioned above is expected to be much higher than the present case, leading to higher reactivity of monomers. The probability of radical–monomer interaction (resulting in generation of monomeric radicals) in such situations is also higher and it is perhaps for these reasons that Bradley et al. [19] could achieve copolymerization without addition of external initiator.

Another possible reason for the discrepancy between our results with those reported in previous literature is the gas sparging protocol during copolymerization. In the copolymerization experiments of Bahattab et al. [25,26] and Bradley et al. [19], argon was passed *through* the reaction mixture *during* sonication, while in the present study the reaction mixture was purged with gas (either argon or nitrogen) *prior* to sonication. This procedure strips out all dissolved oxygen and leaves small gas bubbles in the medium that could provide nuclei for cavitation events. No gas was sparged through reaction mixture during sonication. Sparging of gas (especially monatomic gas such as argon) during sonication sharply increases the population of cavitation nuclei in the medium, and hence, the net production of radicals through transient collapse (T.G. Leighton, personal communication). As against this, the population of cavitation bubbles, and hence, the production rate of radicals through cavitation in our experiments is expected to be much lesser than those of Bahattab et al. [25,26] and Bradley et al. [19].

To summarize, the reactivity ratios of BA and MMA observed in the present study, viz. $r_{MMA} = 0.2408$ & $r_{BA} = 0.2036$ for argon sparged solutions, and $r_{MMA} = 0.2848$ and $r_{BA} = 0.0755$ for nitrogen sparged solutions, are significantly different than those reported in previous literature, viz. $r_{BA} = 0.36$ & $r_{MMA} = 2.55$ by Bradley et al. [19] and $r_{BA} = 0.72$ & $r_{MMA} = 3.66$ by Bahattab et al. [25,26]. We attribute this discrepancy to the difference in radical production rate in the medium through transient collapse of cavitation bubbles – either due to difference in the ultrasound intensity or gas sparging protocol or both.

5. Conclusion

The present study tries to get, at least qualitatively, physical insight into the sonochemical copolymerization process using MMA and BA as model monomers. The experimental results have been coupled to simulations of cavitation bubble dynamics. The concurrent analysis of experimental and simulations results have brought forward several important aspects of sonochemical copolymerization process for low to moderate ultrasound intensities, which have been summarized below:

(1) The role of cavitation in the present study is found to be only of physical nature in that it creates emulsification of the reaction mixture and decomposition of external initiator occurs in the thin layer of liquid surrounding the bubble that gets heated to few hundred degrees during transient collapse of the bubble. No role of radicals generated from cavitation bubbles is seen in the copolymerization process.
(2) The reactivity ratios of both monomers have been found to be less than 1 indicating that copolymerization behavior is *moderate* alternating.
(3) The composition of copolymer is different than that in the monomer feed (or in the reaction mixture). For MMA:BA weight ratio of 1:4 and 2:3, the MMA content of copolymer is higher than in the monomer reaction mixture, while for weight ratio of 4:1, opposite result is obtained. This is attributed to limiting reactant (among radicals generated from cavitation bubbles and monomer molecules) and higher reactivity ratio of MMA than BA.

(4) The molecular weight of copolymer is found to reduce with greater fraction of MMA in the monomer feed. This is essentially a consequence of nature of termination of the monomers of BA (i.e. combination) and MMA (i.e. disproportionation).

Acknowledgement

We gratefully acknowledge valuable discussions with Prof. Franz Grieser and Dr. M. Ashokkumar (Univ. of Melbourne) regarding copolymerization protocols and with Prof. T.G. Leighton (Univ. of Southampton) regarding externally seeded gas nuclei for cavitation. We are also thankful to both referees of this paper for their meticulous evaluation of the manuscript and constructive criticism that has contributed to improvement of the manuscript quality.

Appendix A

1. Calorimetric determination of ultrasound intensity and pressure amplitude in reaction mixture

In any ultrasound reactor (either probe type or bath type), actual ultrasound energy delivered to the medium is different from the power setting of the equipment. This is mainly a result of mismatch of electrical impedance and the specific acoustic impedance of the medium (given as product of density of the medium and the sonic velocity in the medium). An easy yet effective method of determination of the actual ultrasound power input to the medium is calorimetry. This method is based on the assumption that all of the energy delivered to the reaction medium is dissipated as heat. We have described this method in one of our earlier papers [41], but for the convenience of the reader we reproduce here.

100 mL water (Millipore, Model: Elix 3) was sonicated in a glass beaker for 10 min with power control knob of sonicator set at 20% of maximum power (500 W), which corresponds to a theoretical power input of 100 W. For 10 min of sonication the temperature of water increased by 1.5 °C. This would mean that the actual rate of energy input to the system was:

$$\frac{mc_p\Delta T}{t} = \frac{0.1 \times 4180 \times 1.5}{600}\frac{\text{Joule}}{\text{s}} = 1.045\ \text{W}$$

The tip of ultrasound horn had a diameter of 13 mm, and thus, the acoustic intensity is calculated as: I= Actual power (W)/Area of horn tip (m^2)=1.045/π/4 $(13\times10^{-3})^2$ =7873 W/m^2 or 0.7873 W/cm^2(≈0.8 W/cm^2).

The relation between acoustic intensity and acoustic pressure amplitude is given as: $I = P_A^2/2\rho c$, where ρ is the density of the medium (i.e. water) and c is the speed of sound in the medium. With substitution of $\rho = 1000$ kg/m^3 and $c = 1481$ m/s, the acoustic pressure amplitude is calculated as:

$$P_A = \sqrt{2I\rho c} = \sqrt{2 \times 7873 \times 1481 \times 1000} = 1.527 \times 105$$
$$\text{Pa} = 1.527\ \text{bar} \approx 1.5\ \text{bar}.$$

2. Method of Bradley and Grieser [12] for determination of monomer conversion

Small aliquot of reaction mixture (~5 mL) was removed after completion of sonication and addition of the inhibitor. This sample was dried in ambient air (at temperature of 30 °C) for about 4–5 h, which left behind only polymer and surfactant, after evaporation of water and unreacted monomer. Assuming that the sample was homogeneous (i.e. with same concentration of unreacted monomer and surfactant as in bulk reaction mixture), correction was made for the weight of surfactant in the sample, thereby giving the weight of polymer (per volume of sample). The weight of polymer in reaction mixture was estimated by multiplying the weight of polymer in sample by the volume ratio of reaction mixture and the sample, i.e. by a factor given as (volume of reaction mixture/volume of sample). To this, weight of the polymer attached to the sonicator probe tip (removed using a spatula) is added to yield the total weight of polymer formed in the reaction. The overall conversion of monomer is obtained by dividing the total weight of polymer by the total initial weight of monomers in the reaction mixture.

Supplementary data

Supplementary data associated with this article can be found in the on-line version, at doi:10.1016/j.polymer.2010.05.011.

References

[1] Price GJ. Ultrasonics Sonochemistry 1996;3(3):S229–38.
[2] Price GJ. Ultrasonics Sonochemistry 2003;10(4–5):277–83.
[3] Lindstrom O, Lamm O. Journal of Physical and Colloid Chemistry 1951;55:1139–46.
[4] Henglein A, Schulz R. Zeitschrift fur Naturforschung 1952;7B:484–5.
[5] Henglein A. Makromolekulare Chemie 1954;14:15–39.
[6] Kruus P, Patraboy TJ. Journal of Physical Chemistry 1985;89:3379–84.
[7] Kruus P, McDonald D, Patraboy TJ. Journal of Physical Chemistry 1987;89:3041–7.
[8] Price GJ, Norris DJ, West PJ. Macromolecules 1992;25:6447–54.
[9] Biggs G, Grieser F. Macromolecules 1995;28:4877–82.
[10] Cooper G, Grieser F, Biggs G. Journal of Colloid and Interfacial Science 1996;184:52–63.
[11] Ooi SK, Biggs S. Ultrasonics Sonochemistry 2000;7:125–33.
[12] Bradley M, Gieser F. Journal of Colloid and Interfacial Science 2002;251:78–84.
[13] Xia HS, Wang Q, Liao YQ, Xu X, Baxter SM, Slone RV, et al. Ultrasonics Sonochemistry 2002;9:151–8.
[14] Price GJ, Lenz EJ, Ansell CWG. European Polymer Journal 2002;38:1531–6.
[15] Zhang C, Wang Q, Xia H, Qiu G. European Polymer Journal 2002;39:1769–76.
[16] Yin N, Chen K, Kang W. Ultrasonics Sonochemistry 2006;13:345–51.
[17] Teo BM, Prescott SW, Ashokkumar M, Grieser F. Ultrasonics Sonochemistry 2008;15(1):89–94.
[18] Zheng Y, Cao Y, Pan G. Ultrasonics Sonochemistry 2008;15(4):314–9.
[19] Bradley MA, Prescott SW, Schoonbrood HAS, Landfester K, Grieser F. Macromolecules 2005;38(15):6346–51.
[20] Fujiwara H, Izutsu K, Osaka Kogyo, Daigaku Kiyo. Rikohen 2004;49(1):1–9.
[21] Zhang C, Cao Y, He Y. Journal of Applied Polymer Science 2004;94:763–8.
[22] Yin N, Chen K. Polymer 2004;45(11):3587–94.
[23] Yan L, Wu H, Zhu Q. Green Chemistry 2004;6(2):99–103.
[24] Isayev AI. Elastomer 2003;38(1):38–50.
[25] Bahattab MA, Stoffer JO. Polymer Materials Science and Engineering 2001;85:76–7.
[26] Bahattab M, Stoffer JO, Forcinitti D. Polymer Chemistry 2002;43(2):1031–2.
[27] Liu J, Chen K, Li Z. Polymer Journal (Tokyo) 2000;32(2):103–6.
[28] Koda S, Amano T, Nomura H. Ultrasonics Sonochemistry 1996;3(2):S91–5.
[29] Fujiwara H, Tanaka J, Horiuchi A. Polymer Bulletin (Berlin) 1996;36(6):723–8.
[30] Chen K, Chen S, Xu X. Journal of Macromolecular Science 1992;A29(1):55–64.
[31] Price GJ, Daw MR, Newcombe NJ, Smith PF. British Polymer Journal 1990;23(1–2):63–6.
[32] Young FR. Cavitation. London: McGraw Hill; 1989.
[33] Leighton TG. The acoustic bubble. San Diego: Academic Press; 1994.
[34] Hart EJ, Henglein A. Journal of Physical Chemistry 1985;89(20):4342–7.
[35] Hart EJ, Henglein A. Journal of Physical Chemistry 1987;91(13):3654–6.
[36] Colussi AJ, Weavers LK, Hoffmann MR. Journal of Physical Chemistry A 1998;102(35):6927–34.
[37] Yasui K. Physical Review E 1997;56:6750–60.
[38] Storey BD, Szeri AJ. Proceedings of Royal Society of London Series A 2000;456:1685–709.
[39] Suslick KS. Science 1990;247:1439–45.
[40] Morya NK, Iyer PK, Moholkar VS. Polymer 2008;49:1910–25.
[41] Sivasankar T, Paunikar AW, Moholkar VS. AIChE Journal 2007;53(5):1132–43.
[42] Grassie N, Torrance BJD, Fortune JD, Gemmell JD. Polymer 1965;6:653–8.
[43] Odian G. Principles of polymerization. 3rd ed. New York: John Wiley & Sons; 1991.
[44] Fineman M, Ross SD. Journal of Polymer Science 1950;5:259–62.
[45] Atchley AA, Prosperetti A. Journal of Acoustical Society of America 1989;86:1065–84.

[46] Prasad Naidu DV, Rajan R, Kumar R, Gandhi KS, Arakeri VH, Chandrasekaran S. Chemical Engineering Science 1994;49(6):877–88.
[47] Yasui K, Iida Y, Tuziuti T, Kozuka T, Towata A. Physical Review E 2008;77. 016609–1-016609-10.
[48] Ilyichev VI, Koretz VL, Melnokov NP. Ultrasonics 1989;27:357–61.
[49] Rajan R, Kumar R, Gandhi KS. Chemical Engineering Science 1998;53:255–71.
[50] Storey BD, Szeri AJ. Proceedings of Royal Society of London Series A 2001;457:1685–700.
[51] Krishnan SJ, Dwivedi P, Moholkar VS. Industrial and Engineering Chemistry Research 2006;45:1493–504.
[52] Kamath V, Prosperetti A, Egolfopoulos FN. Journal of Acoustical Society of America 1993;94:248–60.
[53] Sochard S, Wilhelm AM, Delmas H. Ultrasonics Sonochemistry 1997;4: 77–84.
[54] Gong C, Hart DP. Journal of Acoustical Society of America 1998;104: 2675–82.
[55] Colussi AJ, Hoffmann MR. Journal Physical Chemistry A 1999;103:11336–9.
[56] Moss WC, Young DA, Harte JA, Levalin JL, Rozsnyai BF, Zimmerman GB, et al. Physical Review E 1999;59:2986–92.
[57] Toegel R, Gompf B, Pecha R, Lohse D. Physical Review Letters 2000;85: 3165–8.
[58] Kumar KS, Moholkar VS. Chemical Engineering Science 2007;62:2698–711.
[59] Keller JB, Miksis MJ. Journal of Acoustical Society of America 1980;68: 628–33.
[60] Prosperetti A, Lezzi A. Journal of Fluid Mechanics 1986;168:457–77.
[61] Brennen CE. Cavitation and bubble dynamics. Oxford: Oxford University Press; 1995.
[62] Hirschfelder JO, Curtiss CF, Bird RB. Molecular theory of gases and liquids. New York: Wiley; 1954.
[63] Condon EU, Odishaw H. Handbook of physics. New York: McGraw Hill; 1958.
[64] Reid RC, Prausnitz JM, Poling BE. Properties of gases and liquids. New York: McGraw Hill; 1987.
[65] Bird RB, Stewart WE, Lightfoot EN. Transport phenomena. 2nd ed. New York: Wiley; 2001.
[66] Grossmann S, Hilgenfeldt S, Zomack M, Lohse D. Journal of Acoustical Society of America 1997;102:1223–7.
[67] Press WH, Teukolsky SA, Flannery BP, Vetterling WT. Numerical recipes. 2nd ed. New York: Cambridge University Press; 1992.
[68] Prosperetti A, Commander KW. Journal of Acoustical Society of America 1989;85:732–46.
[69] Fyrillas M, Szeri AJ. Journal of Fluid Mechanics 1994;277:381–407.
[70] Lofstedt R, Weninger K, Puttermann SJ, Barber BP. Physical Review E 1995;51:4400–10.
[71] Eriksson G. Chemica Scripta 1975;8:100–3.
[72] Neppiras EA. Physics Reports 1980;61:159–251.
[73] Landfester K. Macromolecular Rapid Communications 2001;22:896–936.
[74] Toegel R. Reaction–diffusion kinetics of a single sonoluminescing bubble. Ph. D. Dissertation. Enschede:Twente University Press; 2002.